sustainability

MDPI

Article

Comprehensive Comparative Analysis of Morphology Indexes for Solar Radiation Acquisition Potential in Lhasa Urban Residential Area

Guorui Song [1], Yu Liu [1,*], Wenqiang Li [2], Jingbo Tan [3] and Seigen Cho [4]

[1] School of Mechanics, Civil Engineering and Architecture, Northwestern Polytechnical University, Xi'an 710129, China; songguorui@mail.nwpu.edu.cn
[2] Digitalize Civil Branch of China Railway 12th Bureau Co., Ltd., Xi'an 710076, China; zihuogoe@163.com
[3] School of Architecture, South China University of Technology, Guangzhou 510641, China; tan_juhan@126.com
[4] Institute of Urban Innovation, Yokohama National University, Yokohama 240-8501, Japan; zhang39@gmail.com
* Correspondence: liuyu@nwpu.edu.cn

Abstract: Solar energy is a type of renewable and sustainable energy. Enhancing the acquisition and utilization of solar radiation in urban residential areas is a crucial strategy for advancing sustainable development goals. The morphology of urban residential areas plays a vital role in determining their solar radiation acquisition (SRA) potential. Existing studies have primarily focused on exploring the correlation between the individual morphology index and SRA potential for residential areas. However, in the actual process of project design, there is a common need to simultaneously adjust multiple morphology indexes according to specific criteria. The question of "How to compare the magnitude of the impact of simultaneous changes in multiple morphology indexes on the SRA potential of a residential area" has not yet been systematically analyzed and fully answered. This study compares the sensitivity of multiple morphology indexes when changed collectively and assesses their comprehensive impact on the SRA potential of residential areas. The aim is to determine how to comprehensively control multiple morphology indexes in the early planning and design stages to maximize solar energy utilization in residential areas. It is concluded that, when considering the floor area ratio index under identical conditions, an increase in building density proves more advantageous for enhancing SRA compared to an increase in building height. In cases where the building height is less than 24 m and the floor area ratio is below 1.5, elevating the building density yields greater photovoltaic (PV) potential for the residential area. With a limited site area, the impact of building height on SRA far outweighs that of the layout. The layout does not significantly affect the annual solar radiation amount per unit of external surface area (ASU). With increasing building height, the impact of layout on heating season solar radiation amount per unit of external surface area (HSU) becomes more pronounced. A vertical staggered layout and a row layout exhibit significantly superior performance compared to a horizontal staggered layout in this regard. However, when the building height exceeds 24 m and the floor area ratio surpasses 1.5, the PV potential of the vertical staggered layout surpasses that of the row layout and horizontal staggered layout for the same building height. The influence of building height on SRA is slightly greater than that of the building orientation under similar conditions. The change in SRA potential with orientation under the same height follows a consistent pattern.

Keywords: solar radiation acquisition potential; residential area morphology; BP neural network; comprehensive comparative analysis; sustainable development

check for updates

Citation: Song, G.; Liu, Y.; Li, W.; Tan, J.; Cho, S. Comprehensive Comparative Analysis of Morphology Indexes for Solar Radiation Acquisition Potential in Lhasa Urban Residential Area. *Sustainability* **2024**, *16*, 4893. https://doi.org/10.3390/su16124893

Academic Editor: Jianming Cai

Received: 30 April 2024
Revised: 1 June 2024
Accepted: 3 June 2024
Published: 7 June 2024

Copyright: © 2024 by the authors. Licensee MDPI, Basel, Switzerland. This article is an open access article distributed under the terms and conditions of the Creative Commons Attribution (CC BY) license (https://creativecommons.org/licenses/by/4.0/).

1. Introduction

Climate change is causing widespread damage to the achievement of the sustainable development goals. The development of solar radiation technologies can reduce the

dependence of buildings on fossil energy sources, thereby mitigating climate change by reducing greenhouse gas emissions. Residential buildings are one of the most important and numerous building types in cities [1]. Urban residential areas have great potential and many advantages for solar radiation development [2,3]. To utilize solar radiation in a building, the external surfaces of the building must acquire sufficient solar radiation.

Lhasa (29°41′ N, 91°1′ E), situated at an altitude of 3650 m in the heart of the Tibetan plateau, experiences cold winters necessitating the use of heating systems to maintain a comfortable indoor environment [4]. The heating load is substantial, and local traditional energy sources are relatively scarce. Despite these challenges, Lhasa is endowed with abundant solar resources, boasting more than 3000 h of sunshine annually. With a low latitude and minimal atmospheric cloud cover, the region receives up to 8400 MJ/m^2 of solar radiation per year [5]. Given this solar richness, Lhasa holds immense potential and a compelling necessity to develop solar energy utilization technology. Both national and local governments actively promote policies to guide the development of solar buildings in the region.

The morphology of building complexes within residential areas directly impacts the accessibility of solar radiation in those areas, consequently influencing solar radiation acquisition. With the rapid urbanization in Lhasa, the density of buildings is increasing, leading to a reduction in their access to solar radiation. In recent years, scholars have studied how to maximize solar radiation acquisition (SRA) potential through changes in the individual morphology index of residential areas. However, in the actual process of project design, there is a common need to simultaneously adjust multiple morphology indexes according to specific criteria. In response to this question, this study compares the sensitivity of multiple morphology indexes when changed collectively and assesses their comprehensive impact on the SRA potential of residential areas.

2. Existing Research

Research on the comparison of the sensitivity of multiple morphology indexes, when changed collectively regarding the SRA potential of residential areas, is currently categorized into two main branches. The first part involves the study of morphology indexes in actual residential areas based on their SRA potential. This type of study typically selects actual residential areas as the subject of investigation. By examining the morphology of established urban residential areas, researchers explore the relationship between morphology indexes related to SRA potential.

Lu et al. concluded that the point layout (a uniform "dot" distribution with square buildings) is superior to the slab layout (a "linear" distribution with rectangular buildings) in terms of sunlight acquisition, with the hybrid layout (a mix of the "dot" distribution and the "linear" distribution with both square and rectangular buildings) falling in the middle [6]. Košir et al. concluded that building density and building orientation are the most important indexes affecting the number of daylight hours [7]. Martins et al. concluded that the aspect ratio and building spacing are obtained as more significant indexes affecting solar radiation and insolation on the building surface [8]. Sarralde et al. concluded that changes in residential area morphology indexes have a much greater effect on façade solar radiation (45 per cent) than on roof solar radiation (9 per cent) [9]. Zhu et al. found that the greater the irregular fluctuations in building height, the greater the SRA potential [10]. Liu concluded that the layout of the residential area is better in row layouts, with a regular tessellation preferred (misalignments between rows and columns in the east–west or north–south directions should be minimized) [11]. Chen concluded that the building density, building complex morphology factor, and standard deviation of building height have a strong correlation with the total annual solar radiation [12]. Wu developed three incident solar radiation prediction indexes (ISRPIs) that combine the building height, the building-exterior-area-to-site-area ratio, and the sky view factor. The ISRPI combines the advantages of several traditional urban morphology indexes and exhibits a strong linear relationship method with incident solar radiation under both clear and cloudy weather [13].

Tian concluded that the floor area ratio, building density, average building height, and building spacing have a significant effect on the SRA potential of residential areas, with correlation coefficients of 75%, 71%, 78%, and 72%, respectively [14]. Wen concluded that in order to maximize the solar radiation acquisition potential of the residential areas, horizontal staggered rows are optimal, followed by parallel rows in the layout of the residential areas [15]. Boccalatte et al. concluded that building height, building volume, and the height difference between buildings have a high correlation with the amount of solar radiation from roofs [16]. Zheng concluded that the floor area ratio, building density, and the ratio of total building external surface area to site area have a great impact on SRA in residential areas [17].

The second part focuses on the study of morphology indexes in typical residential areas with parameterized samples. In studies of this nature, residential areas are often used as references, and the typical morphology of residential areas in a given region is extracted through extensive research. Researchers then investigate the impact of residential area morphology indexes on SRA potential by adjusting the morphology control parameters of these typical residential areas.

Vermeulen et al. concluded that urban high-building density areas have easy access to solar radiation, where the courtyard layout maximizes the total radiation of residential areas [18]. Li et al. found that as building density increases, the solar potential of the complex increases [19]. Morganti et al. found that building density, the ratio of the area of the façade to the base, and the sky factor have the most significant relationship with the effect of radiation values [20]. Bai concluded that the building layouts (the parallel determinant, the three-side street style, and the four-side enclosure type), building height, and building orientation have a great influence on solar radiation acquisition [21]. Jiang concluded that the building layout and building density have a small impact on solar potential, while the floor area ratio and building spacing, as well as building morphology, have a large impact on solar potential [22]. Aghamolaei et al. concluded that building height, density, and street width affect SRA in residential area buildings, with building height having the greatest effect [23]. Zhang et al. concluded that under the same planning conditions and design premise, different urban block types can increase the solar radiation harvesting potential and rooftop photovoltaic (PV) capacity by up to 200%. Among them, courtyard and hybrid layouts are superior to other types, especially tower and panel blocks [24]. Zhang concluded that the optimal layout for high-rise residential areas in Lhasa is the vertical staggered layout, and multi-story residential areas require a mixed staggered layout [25].

In summary, there is some current research on the impact of residential area morphology indexes on SRA potential. Scholars have conducted comparative analyses on the influence of individual morphology indexes, such as the building layout, floor area ratio, building density, building height, and building orientation, on residential area SRA by way of control variables. However, architects in the practical design process often need to consider meeting various requirements of the client, rather than simply changing the individual morphology index. Instead, they need to adjust multiple morphology indexes simultaneously to meet the conditions of the site. In this context, it becomes especially important to compare the comprehensive impact of various morphology indexes on the SRA in residential areas and their sensitivity under comprehensive impacts. In this study, urban residential areas in Lhasa, China, were selected as the subject of the study. Although some research has been conducted in areas such as Harbin, Shanghai, and Wuhan in China [11,12,14,15,17,21,22,26–33], there is a distinct lack of research on solar resource-rich areas such as Lhasa and Xining.

3. Research Method

A large sample of residential areas is required as a basis for the study to compare the sensitivity of multiple morphology indexes when changed collectively on the SRA potential of residential areas. A parametric approach was implemented in this study, which facilitates the rapid establishment of numerous morphological scenarios, ensuring

comprehensive coverage of the morphological possibilities observed in typical residential areas. Moreover, it offers flexibility in adjusting morphological variables as necessary to ensure comparability among the scenarios. Traditional methods of obtaining data require first modeling residential areas and then simulating their solar radiation [31]. However, when dealing with numerous high-density residential areas, computational time consumption becomes a major challenge in parametric studies due to the multitude of influencing factors and the extensive data to be processed [26]. Therefore, a BP neural network is constructed to reflect the functional relationship between the SRA of the Lhasa residential area and its influencing indexes in this study. The BP neural network is a relatively mature and widely used artificial neural network, which has the advantages of being self-adaptive as well as possessing a self-learning capability, nonlinear mapping, and fault tolerance, and can represent complex functional relationships of internal action mechanisms [34]. The SRA prediction model will greatly simplify the calculation mode of solar radiation simulation using software-based platforms and eliminate the tedious traditional modeling and simulation process. By only adjusting the morphology index data of residential areas, the SRA of residential areas can be quickly and accurately calculated and predicted. The specific process (Figure 1) is illustrated as follows:

1. Residential area archetypes characterization and parameterization. The morphological characteristics and parameters of typical residential areas were extracted and summarized in Lhasa. They were then used as the benchmark for establishing the experimental parametric models. Then residential area morphology indexes and SRA indexes of high correlation were identified. We then utilized Rhinoceros 7.0 modeling software and its parametric modeling platform Grasshopper with Ladybug 1.4.0 to model the residential area and simulate solar radiation.
2. BP neural network constructing. A BP neural network model with morphology indexes as the input layer and SRA indexes as the output layer was constructed. To train and test the BP neural network, the morphology indexes dataset of actual case residential areas and ideal homogeneous residential areas and the corresponding SRA index dataset were used. During training, the neural network iteratively adjusts its parameters (weights and biases) based on the training set to minimize the difference between predicted and actual SRA indexes.
3. Comprehensive comparative analysis. Once the BP neural network is trained and validated, it serves as a prediction model for estimating SRA based on morphology indexes for Lhasa residential areas. A large amount of data was obtained from several calculations using the predictive model. Statistical methods were then used to compare the sensitivity of multiple core morphology indexes such as the floor area ratio, building density, building height, building layout, and building orientation to the effects of SRA.

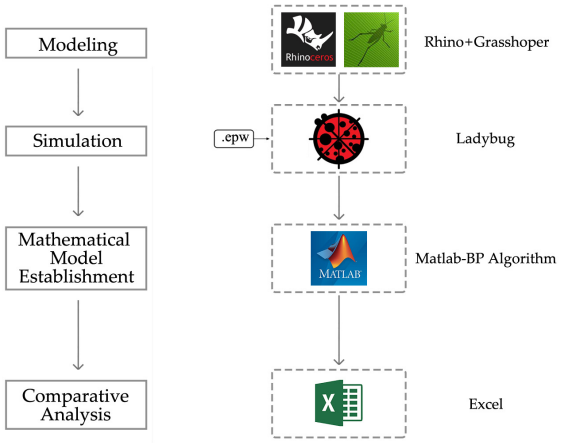


Figure 1. Workflow diagram.

4. Indexes Determination

Based on our research group's preliminary research, eight morphology indexes (Table 1) with high correlations with SRA and four SRA indexes (Table 2) were selected [11,15,35,36]. The annual SRA of residential areas was studied using the annual solar radiation per unit of building external surface area (ASU), combined with the annual solar radiation on the total building external surface area; the solar radiation per unit of external surface area in the heating season (HSU), combined with the solar radiation on the total building external surface area in the heating season, was used to study the SRA of residential areas in the heating season. Citing the annual solar radiation threshold per unit area (800 kW·h $(m^2 \cdot a)^{-1}$) corresponding to different solar energy utilization technologies proposed by R. Compagnon [37], the PV potential of the building is analyzed in a comprehensive manner using two indexes: the percentage of external surface area above the threshold of solar radiation of the residential area building complex to the total external surface area (SA_{800}), and the percentage of radiation above the threshold to the total radiation (SS_{800}).

Table 1. The 8 morphology indexes of residential area.

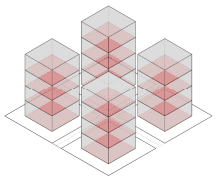
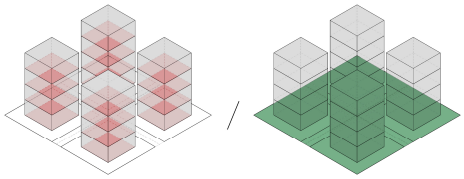
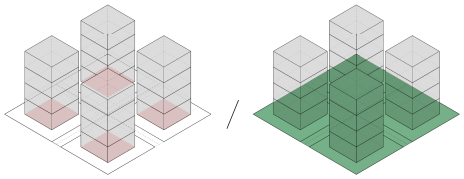
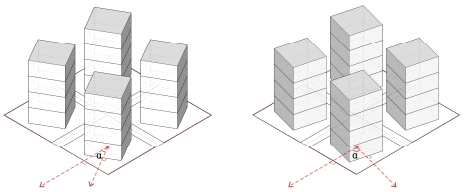
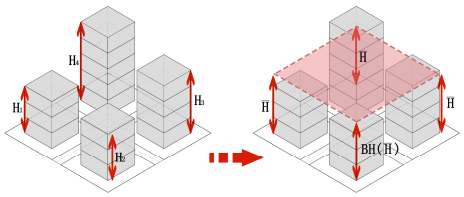
Morphology Index	Calculation Method	Schematic	Note
Gross Floor Area (GFA)	The sum of the horizontal projections of the buildings on each floor of the site		
Floor Area Ratio (FAR)	$FAR = \frac{\text{Gross Floor Area}}{\text{Site Area}}$		An important index of construction land use intensity.
Building Density (BD)	$BD = \frac{\text{Building Footprint area}}{\text{Site Area}}$		
Building Orientations (BO)	The front façade of a building, or the direction faced by the main façade of a building.		The main façade refers to the south façade where the main rooms are located.
Building Height (BH)	$BH = \frac{\text{Gross Floor Area}}{\text{Building Footprint Area}}$		

Table 1. *Cont.*

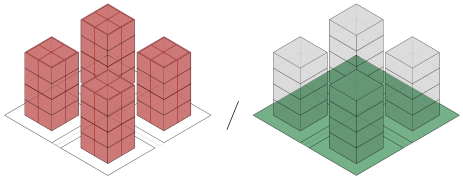
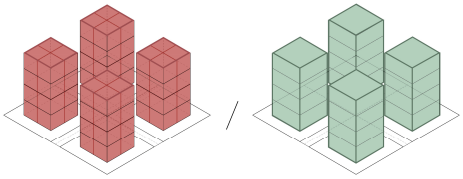
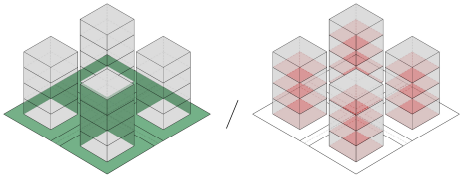
Morphology Index	Calculation Method	Schematic	Note
Building Surface Complexity (STL)	$STL = \frac{\text{Building Total External Surface Area}}{\text{Site Area}}$		Indicates the amount of external building surface occupied per unit of site area.
Building Complex Morphology Factor (QTX)	$QTX = \frac{\text{Building Total External Surface Area}}{\text{Building Total volume}}$		Similar expressions of the shape coefficient of monolithic buildings at the group level.
Open Space Ratio (OSR)	$OSR = \frac{\text{Unbuilt Area}}{\text{Gross Floor Area}}$		Its value can indirectly reflect the degree of mutual shading of buildings.

Table 2. The 4 SRA indexes.

Potential Index	Calculation Method	Note
Annual Solar Radiation Amount per Unit External Surface Area (ASU)	$ASU = \frac{\text{Annual Solar Radiation Amount Building Received}}{\text{Building Total External Surface Area}}$ (unit: $kW{\cdot}h(m^2{\cdot}a)^{-1}$)	ASU refers to the ratio of the solar radiation acquired by the external surface of a single unit or group of buildings to the total external surface area of the building in a year. The larger the value of this performance index, the more efficient the corresponding building complex or building unit is in terms of SRA. The combination of this index and the total amount of solar radiation a building receives in a year provides a more comprehensive picture of a building's potential to obtain solar radiation throughout the year.
Heating Season Solar Radiation Amount per Unit External Surface Area (HSU)	$HSU = \frac{\text{Heating Season Solar Radiation Amount Building Received}}{\text{Building Total External Surface Area}}$ (unit: $kW{\cdot}h(m^2{\cdot}a)^{-1}$)	HSU refers to the ratio of the total solar radiation acquired by the external surfaces of a building to the total external area of the building during the duration of the local heating season. Characterize the ability of residential area and building units to obtain solar radiation during the heating season. It is necessary to analyze this index in Lhasa, which is a cold region (climate zone VI) of the building thermal/climatic zoning, with cold winters and large heating demand, and cooler summers without air conditioning and cooling demand. The larger the value of this performance index, the higher the efficiency of SRA for the heating season of the corresponding building complex or building unit. This index combined with the total amount of solar radiation obtained by a building during the heating season provides a more comprehensive picture of a building's potential for SRA during the heating season.

Table 2. *Cont.*

Potential Index	Calculation Method	Note
Ratio of Area with Radiation Exceeding 800 to Total External Surface Area (SA_{800})	$SA_{800} = \frac{\text{Annual Solar Radiation Exceeding 800 kW·h}\left(m^2 \cdot a\right)^{-1} \text{ Amount Building Received}}{\text{Building Total External Surface Area}}$	The thresholds are based on the PV and solar thermal thresholds proposed by R. Compagnon, which focus on the PV potential of buildings [37]. SA_{800} refers to the area of the external surface of a building complex or building unit that acquires solar radiation in excess of the 800 threshold in a year as a percentage of the total external area. SS_{800} refers to the solar radiation acquired by the external surface of a building complex or building element in excess of the 800 threshold in a year as a percentage of the solar radiation acquired by the total annual external surface area.
Percentage of Radiation Exceeding 800 (SS_{800})	$SS_{800} = \frac{\text{Annual Solar Radiation Exceeding 800 kW·h}\left(m^2 \cdot a\right)^{-1} \text{ Amount Building Received}}{\text{Annual Solar Radiation Amount Building Received}}$	

5. Sample Set of Morphology Models

5.1. Actual Case Residential Areas Dataset

In order to select residential areas that are in line with the current situation and future development of Lhasa's residential areas, 81 residential areas were selected from those built after 2010 in Lhasa through online and field research (Figure 2).

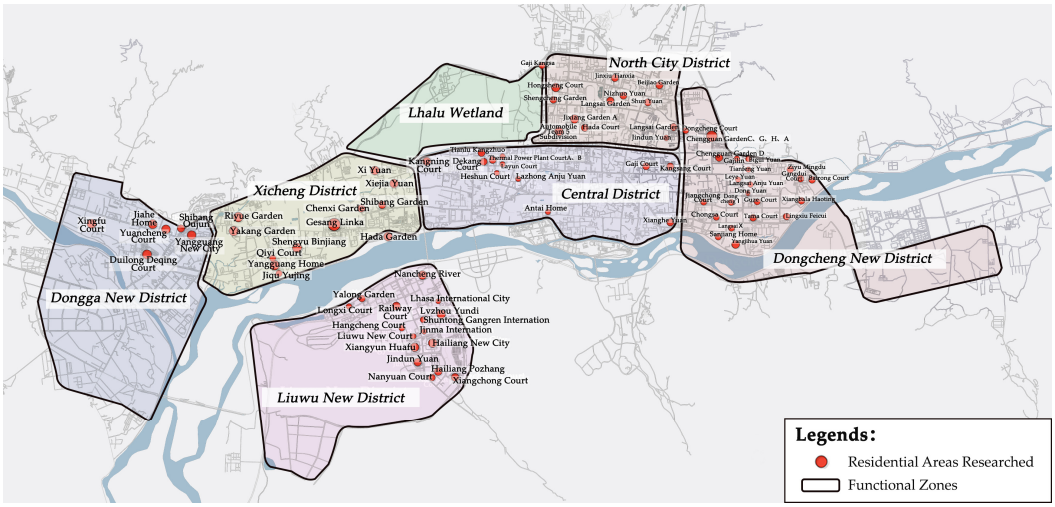


Figure 2. Map of residential areas researched in Lhasa.

According to the research results, the morphological characteristics and parameters of typical residential areas were extracted and summarized in Lhasa (Figure 3). Analysis revealed that the largest proportion of the site area of residential areas in Lhasa is in the range of 5 hm^2 to 10 hm^2, accounting for 40.4% of the total number of residential areas in the research. On the whole, the scale of residential areas in Lhasa is mainly small and medium-sized, and medium-sized and large-sized residential areas are mainly distributed within the scope of several functional new areas. The number of residential areas with floor area ratios in the range of 1.5 to 2.0 is the highest, accounting for 39.8% of the total number of residential areas studied. The overall development intensity of high-rise residential areas in Lhasa is moderate to low. Residential areas in Lhasa with a density of 10–20% accounted for the largest proportion of the total number of residential areas studied, at 48.1%. According to the classification of the layout morphology and statistical analysis, the urban area of Lhasa has a larger proportion of the total number of investigations with hybrid (a combination of horizontal staggered rows and vertical staggered rows) and row layouts, which is also conducive to the acquisition and use of solar energy by buildings. Residential buildings in Lhasa are mainly multi-story Type I (4~6 storys) and high-rise Type

I (10~18 storys). In the analysis of the orientation of the existing residential buildings in Lhasa, it is concluded that the number of existing residential buildings in Lhasa facing south is the largest, accounting for 45.6% of the number of single-unit residential buildings in the study. The database of actual cases was obtained by modeling the specific values of eight morphology indexes for the eight selected residential area morphology indexes and the specific values of the corresponding four SRA indexes. Table 3 shows 10 of these datasets.

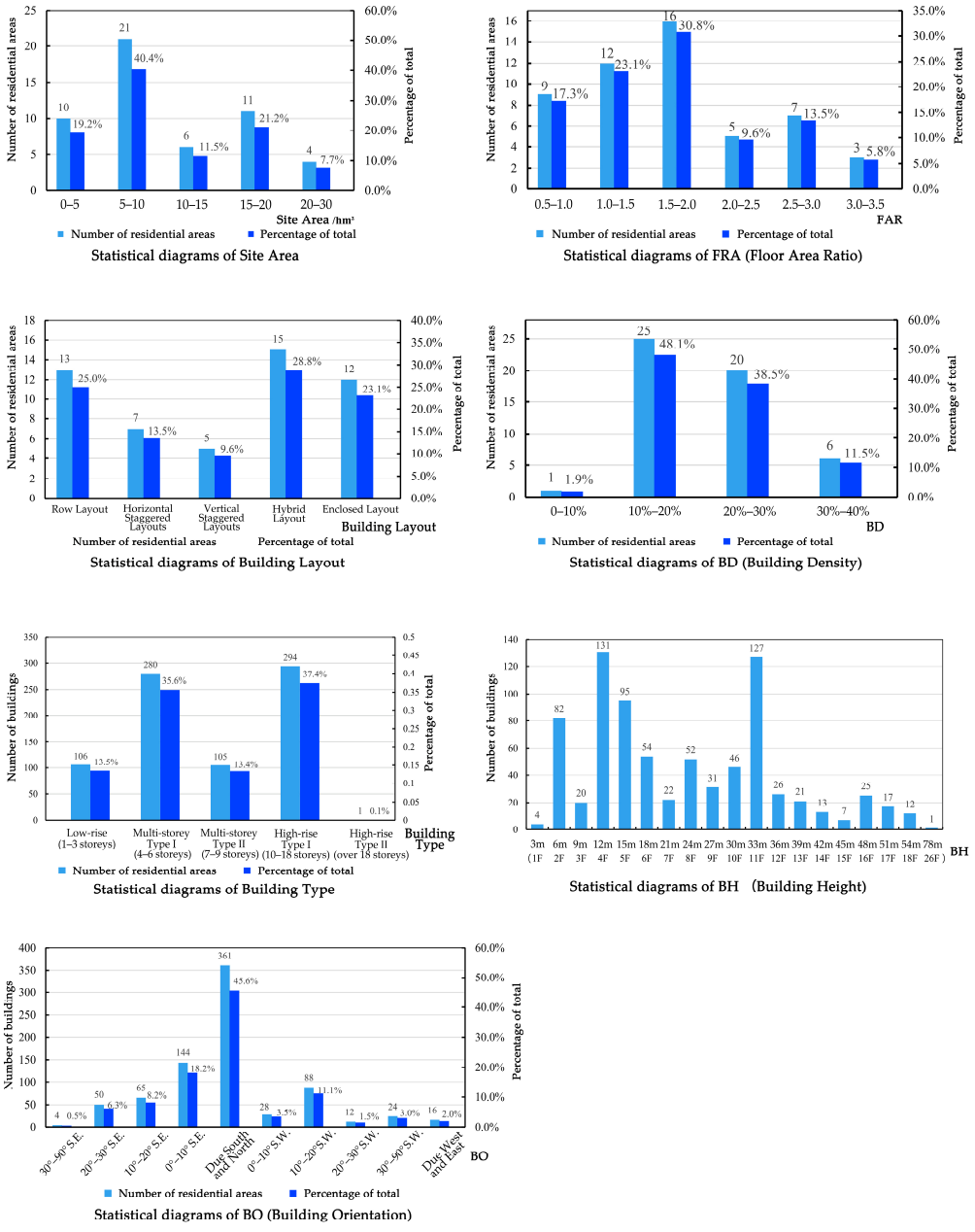


Figure 3. Statistical diagrams of morphology indexes of residential areas researched in Lhasa.

Table 3. Selected data extracted from the actual case sample library. (1) List of independent variables (list of morphology index values). (2) List of dependent variables (list of values of solar radiation indexes).

(1)								
Number	**GFA (m^2)**	**FAR**	**BD (%)**	**BO (°)**	**BH (m)**	**STL**	**QTX**	**OSR**
1	119,610.50	0.87	10.60	−4.3	24.41	0.84	0.320	1.023
2	168,630.95	1.77	14.47	−4.2	40.09	1.13	0.212	0.482
3	297,822.80	1.95	12.30	−4.5	45.88	1.22	0.208	0.449
4	98,436.38	2.95	22.33	−23.3	39.67	2.22	0.251	0.263
5	33,268.30	1.04	17.45	0.5	15.00	0.79	0.255	0.795
6	16,329.49	2.08	23.14	0.5	27.00	1.53	0.244	0.369
7	47,558.15	1.02	25.44	0.0	12.00	0.93	0.306	0.733
8	28,652.81	1.25	32.68	0.0	11.50	1.07	0.285	0.537
9	37,045.13	0.88	21.98	0.0	12.00	0.90	0.340	0.888
10	21,149.48	1.04	26.07	0.0	12.00	1.08	0.345	0.709

(2)				
Number	**ASU ($kW \cdot h(m^2 \cdot a)^{-1}$)**	**HSU ($kW \cdot h(m^2 \cdot a)^{-1}$)**	**SA_{800}**	**SS_{800}**
1	687.13	263.78	0.377	0.738
2	673.43	248.09	0.357	0.696
3	667.31	263.17	0.362	0.684
4	613.83	213.96	0.262	0.586
5	903.74	328.12	0.475	0.766
6	829.33	300.98	0.444	0.723
7	949.23	338.64	0.472	0.790
8	968.44	328.14	0.433	0.759
9	890.41	310.83	0.424	0.778
10	868.73	302.04	0.418	0.801

5.2. Ideal Homogeneous Residential Areas Dataset

In order to control the variables to make the study results essential, a sample library of ideal homogeneous residential areas with the same plan form and height of single buildings and uniform spatial distribution was constructed.

Based on the results of the research and analysis of the morphology of existing residential areas in Lhasa city, the basic pattern of homogeneous residential areas is determined in terms of the layout of the Lhasa residential area, the width and depth scale of a single building, etc. On this basis, changes in morphology indexes are added, and finally, a large number of parametric samples of homogeneous residential areas with different morphologies are constructed.

A square base of 300 m × 300 m is selected to establish a homogeneous residential area model. In order to match the real urban environment, the parameterized samples of these residential areas are each replicated into a 3 × 3 matrix, and the urban road between residential areas is set to be 30 m wide. Due to the influence of regional climatic conditions, most of the building forms of urban residential areas in Lhasa city are slab type, with tower-type buildings being rarer, and the whole row of local slab collection houses are mostly approximately 55–60 m in width and 12–15 m in depth. Therefore, the study takes the median value and takes the rectangular plan of 57.5 m × 13.5 m as the typical plan form

of single buildings with a 3 m floor height, a uniform distribution, and consistent height. The minimum building spacing is based on the provisions of Article 5.2.2 of the Building Design Fire Code GB 50016-2014 (2018 edition), and the fire spacing of 13 m is taken as the minimum spacing for high-rise civil buildings of the first and second fire ratings. At the same time, to meet the provisions of Article 49 of the Lhasa City Planning Regulations, the building spacing coefficient shall not be less than 1:1.25; building setback land and road red line distance are in accordance with the provisions of Article 51 and Article 64 of the Lhasa City Planning Regulations to determine the setback land red line at 15 m.

A sample containing 2304 homogeneous residential areas was established by changing the building layout (the row layout, the vertical staggered layout, and the horizontal staggered layout), building height (12 m, 18 m, 24 m, 30 m, 54 m, and 78 m), number of building rows and building columns, and building orientation (60° S.E., 30° S.E., due south and due north, 30° S.W., 60° S.W., due east and due west). The samples with a high density and a high floor area ratio (such as residential areas with 26 stories and 10 rows and 4 columns) that do not meet the daylighting code of Lhasa city were excluded, and finally, a homogeneous model sample database containing 876 groups of data was formed, with the floor area ratio ranging from 0.31 to 2.7, which is in line with the actual research situation of Lhasa residential areas. The details are shown in Table 4.

Table 4. The morphology setting of homogeneous residential area sample.

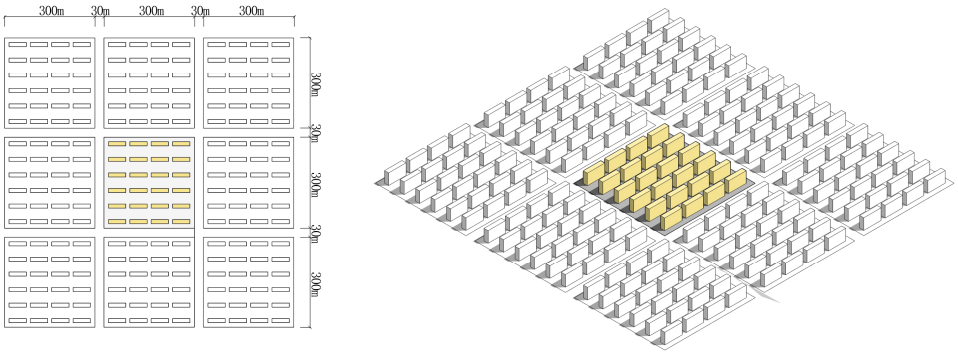
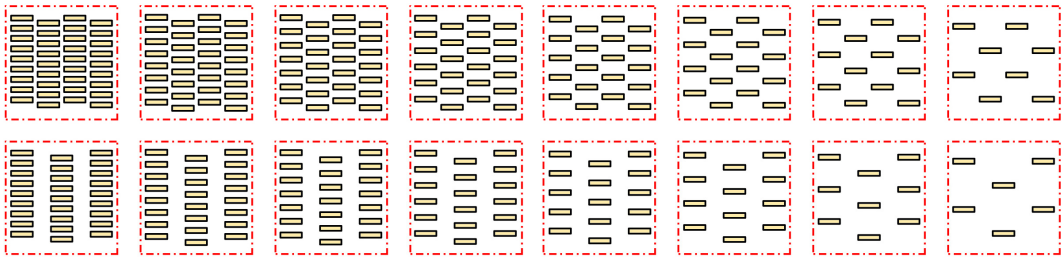
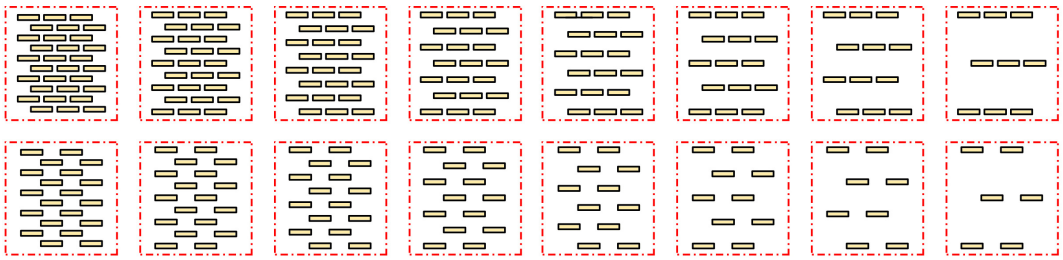
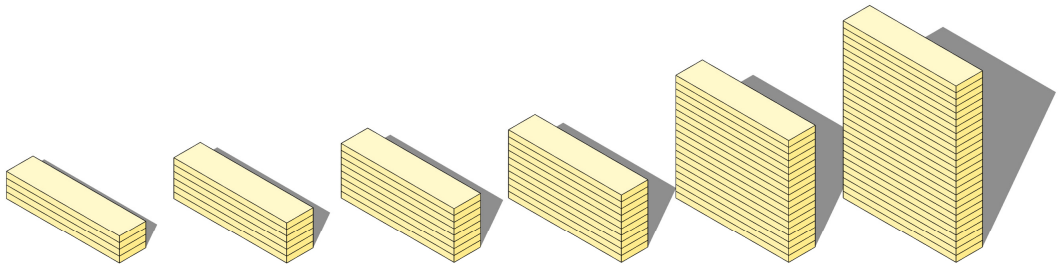
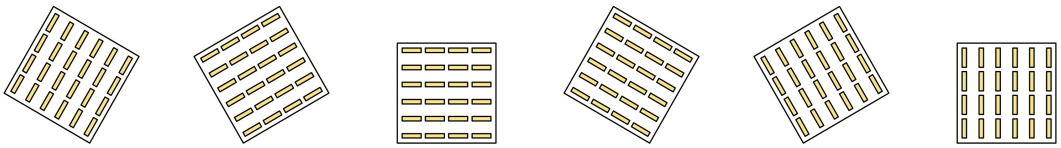
Morphology	Experimental Parametric Scenarios
Residential Area Matrix	
Building Layout	1 Row layouts 

Table 4. *Cont.*

Morphology	Experimental Parametric Scenarios
Building Layout	2 Vertical Staggered Layouts  3 Horizontal Staggered Layouts 
Building Height	 12m (4F) 18m (6F) 24m (8F) 30m (10F) 54m (18F) 78m (26F)
Building Orientation	 60° S.E. 30° S.E. Due South and North 30° S.W. 60° S.W. Due West and East

6. Prediction Model

6.1. Basis and Principle

The residential area solar radiation prediction model is a mathematical model constructed based on the data of the residential area morphology model sample library, in which the input variables of this model are the morphology indexes of the residential area and the output variables are the performance indexes of SRA.

The residential area SRA of residential areas is related to several morphology indexes such as the gross floor area (GFA), floor area ratio (FAR), building density (BD), building orientation (BO), building height (BH), building surface complexity (STL), building complex morphology factor (QTX), open space ratio (OSR), etc. The relationship between these indexes and the residential area SRA of the residential area is a mapping relationship, i.e., for any set of values of the morphology indexes within the building code, the residential area SRA of the residential area has a unique value corresponding to it. Therefore, a BP

neural network model can be developed to represent the mapping relationship between the morphology indexes and the residential area SRA of residential areas.

The BP Neural Network (Back Propagation Neural Network, BPNN) was proposed in 1986 by a group of scientists led by Rumelhart and Mccelland. It is a one-way propagation multilayer feedforward network. With self-learning, self-organization, and excellent non-linear approximation ability, it is one of the most widely used neural network models. The BP neural network consists of an input layer, an output layer, and several hidden layers, and the BP network algorithm is a typical learning process with a teacher. In essence, for the given sample data and error requirements, after establishing the initial network model (including the network structure, the threshold values of the neurons in each layer, and the connection weights between the neurons in each layer), with the goal of reducing the error between the model output value and the sample value, the threshold values of the neurons in each layer of the network and the connection weights between the neurons are repeatedly revised to optimize the model until the error between the model output and the sample value meets the requirement [34]. At this point, the network model reflects the mapping relationship between the variables in the sample data, and the threshold values of the neurons in each layer of the model and the connection weights between the neurons in each layer determine the model output value. We can then use this network model to calculate and predict the SRA of residential areas under different morphology indexes.

6.2. Structure and Training

It has been shown that a BP neural network model with one input layer, one output layer, and one hidden layer, with a hyperbolic tangent S-shaped function for the hidden layer action function and a linear function for the output layer action function, can approximate any continuous multivariate function with arbitrary accuracy when the number of neurons in the hidden layer is appropriate [22]. In this paper, the model structure is established according to this theory (Figure 4). Among them, the input layer has eight neurons, which correspond to eight morphology indexes of residential areas: gross floor area (GFA), floor area ratio (FAR), building density (BD), building orientation (BO), building height (BH), building surface complexity (STL), building complex morphology factor (QTX), and the open space ratio (OSR). The output layer has four neurons corresponding to four SRA indexes: annual solar radiation amount per unit of external surface area (ASU), heating season solar radiation amount per unit of external surface area (HSU), the ratio of the area with radiation exceeding 800 to the total external surface area (SA_{800}), and percentage of radiation exceeding 800 (SS_{800}). The number of neurons in the hidden layer is crucial, as too small of a number will affect the accuracy of model training and prediction and the empirical effect will be reduced; too high of a number will affect the network generalization inference ability. After repeated debugging and comparison with a computer, the number of neurons in the hidden layer was determined to be 40.

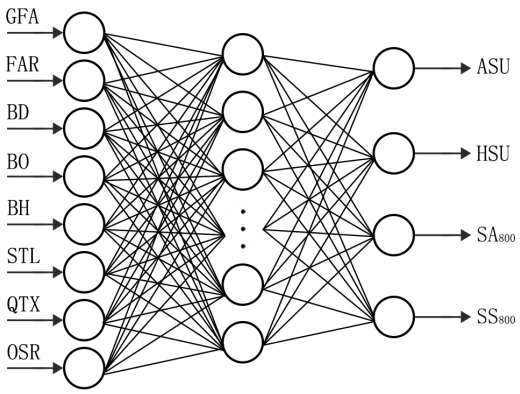


Figure 4. Topology of SRA prediction using BP neural network.

Since the eight morphology indexes and the corresponding SRA indexes have different units of measurement and different orders of magnitude, the model cannot be trained directly using the data in the homogeneous sample database, but should first be normalized, i.e., all the morphology indexes and the corresponding SRA values are transformed into decimals in the interval [0, 1] according to certain rules. After the normalization process, the homogeneous residential area sample data can be used for training the model. The 876 sets of data from the normalized homogeneous residential area sample library were then used to train the model.

In order to subsequently verify the reliability of the resulting model, when the 876 sets of data from the normalized homogeneous model library were imported into the BP neural network for model training, the order of the input variable matrix was first randomly disordered, and then a total of 836 sets of samples from numbers 1 to 836 in the new sequence were selected as the training set, and the remaining 40 sets of samples from numbers 837 to 876 were used as the testing set.

The initial weights and thresholds of the model are taken as random numbers between 0~1. The error level and learning rate are selected, and the program is written in the neural network toolbox in Matlab to train the BP neural network model with 836 sets of sample data. Network training is performed, and the training ends when the learning error reaches the requirement when the training reaches 15,320 times. At this point, the model reflects the mapping relationship between the normalized morphology indexes and the normalized SRA indexes. When the trained model is used to predict the SRA of a residential area, similar to the training model, the morphology index values are first normalized, then the normalized SRA values are calculated using the trained model, and finally, the results are denormalized to obtain the original SRA prediction values.

In order to verify the reliability of the obtained model for the homogeneous sample database, 40 sets of data in the testing set were normalized and imported into the obtained model to obtain the corresponding simulated values of SRA.

Using the sample number of the testing set as the horizontal coordinate, the simulated values of ASU of the testing set are plotted against the measured values (Figure 5a), the simulated values of HSU of the testing set are plotted against the measured values (Figure 5b), the simulated values of SA_{800} of the testing set are plotted against the measured values (Figure 5c), and the simulated values of SS_{800} of the testing set are plotted against the measured values (Figure 5d). It can be seen that the fit between the four output quantities and the output variable system is high, and the R^2 of the fit reaches 0.9823, 0.9875, 0.9786, and 0.9808, respectively. This also proves the accuracy of the present relational model for predicting the SRA of the homogeneous residential area model.

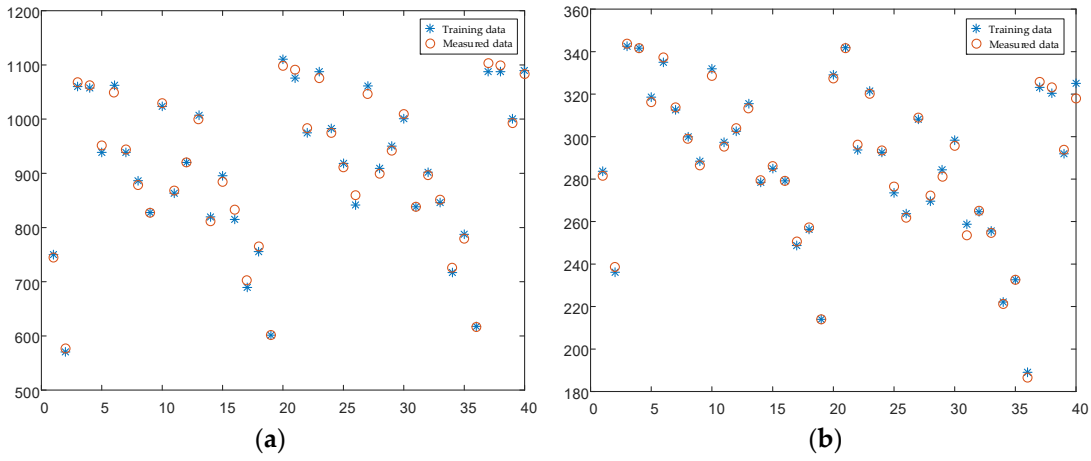


Figure 5. *Cont.*

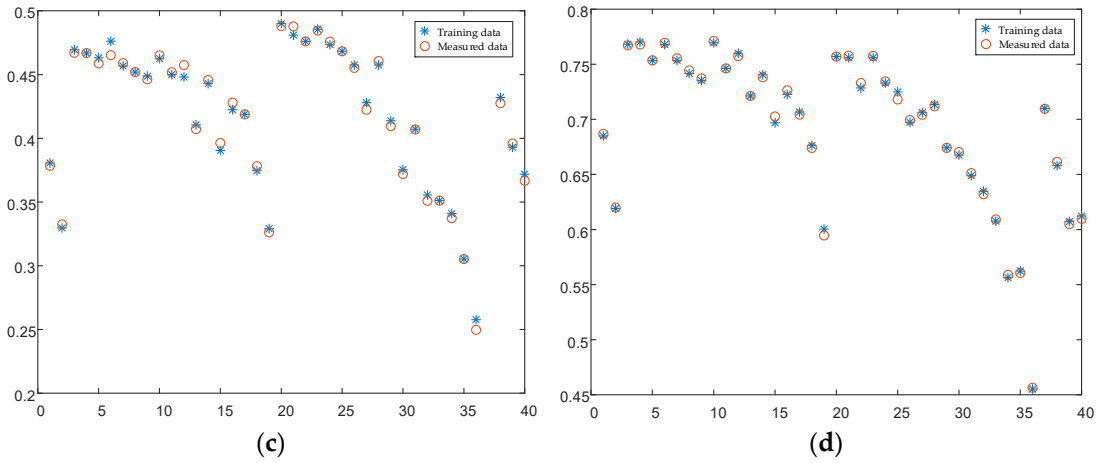


Figure 5. Comparison of simulated and measured values of the testing set in ASU (**a**) and HSU (**b**) and SA_{800} (**c**) and SS_{800} (**d**).

6.3. Verification of the Model

After obtaining a well-fitted model of the relationship between morphology indexes of residential areas and SRA generated by the homogeneous model library, the relationship model is further calibrated using data from the actual case database in order to verify whether the model is still applicable in real cases.

Since the residential area model in the homogeneous model library is too ideal and due to the relationship between the morphology indexes of the residential area and the SRA derived from the data therein alone when imported into the input variable matrix in the actual case, the predicted values of the calculated output variables do not match the actual measured values as well as the predicted values of the homogeneous model, and there are certain deviations. This is mainly because the characteristics of the existing residential areas themselves and the surrounding environment are not the same, and there are multiple external factors that lead to complexity. The R^2 of the fit between the simulated and measured values of ASU (Figure 6a), HSU (Figure 6b), SA_{800} (Figure 6c), and SS_{800} (Figure 6d) in the actual case base are 0.8236, 0.8057, 0.8429, and 0.8966, respectively.

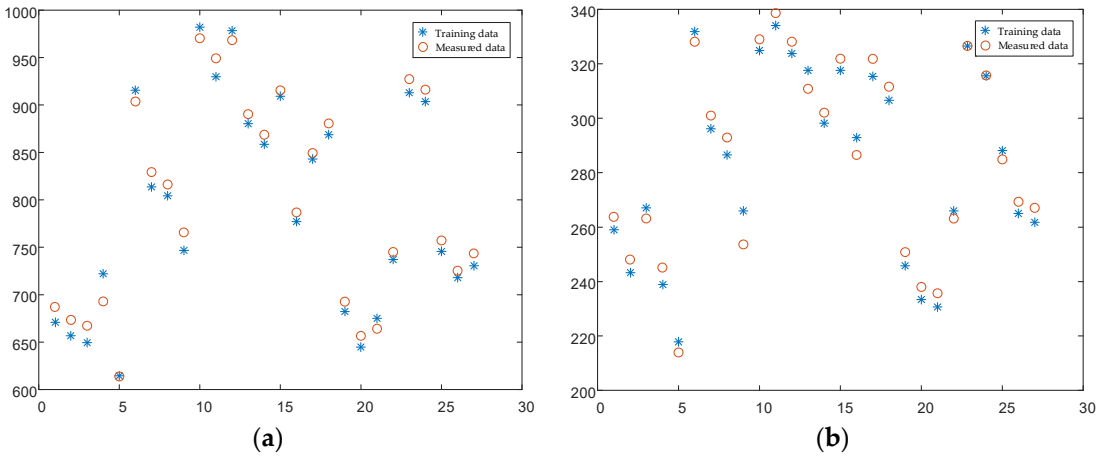


Figure 6. *Cont.*

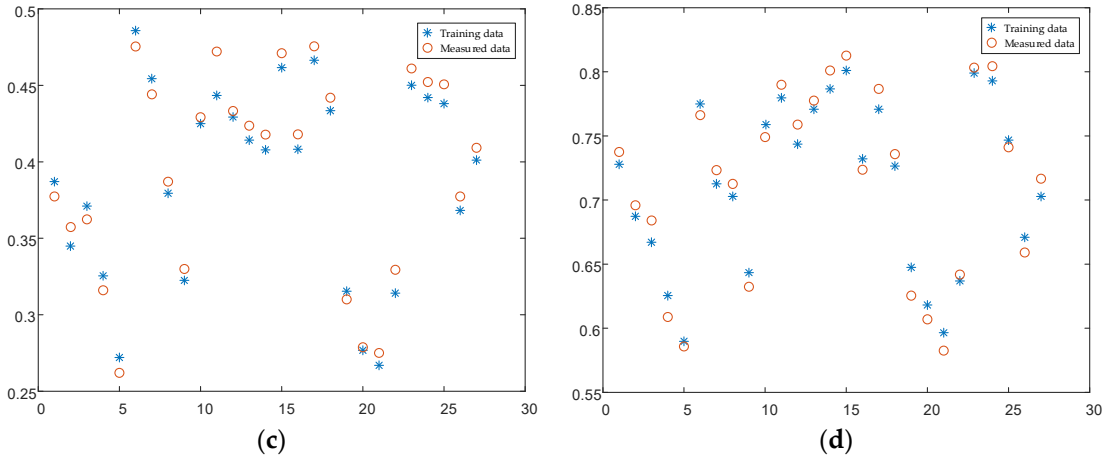


Figure 6. Comparison of simulated and measured values of the actual case in ASU (**a**) and HSU (**b**) and SA_{800} (**c**) and SS_{800} (**d**).

Although there is a certain amount of error in the absolute magnitude of the simulated and measured values, this error is still within the acceptable range, and the overall trend of the simulated values is basically consistent with the overall trend of the measured values. Therefore, it is feasible to use the previously obtained relationship model between the morphology indexes of residential areas and SRA to predict the SRA of actual residential areas.

7. Comparative Analysis of the Indexes

In this section, five morphology indexes, namely, the floor area ratio, building height, building density, layout, and building orientation, which are directly adjusted by architects during the design of residential areas, are selected for further discussion. Their comprehensive impact on the SRA potential of a residential area, when changed collectively, is compared. The discussion below separately explores the influence of building height and building density on residential area SRA, the influence of building layout and building height on residential area SRA, and the influence of building orientation and building height on residential area SRA.

7.1. Effect of Building Density (BD) and Building Height (BH) on SRA

The effects of different floor area ratios on the SRA and photovoltaic (PV) potential of residential areas were selected for comparative analysis under the due south and due north and six typical building heights.

The results show that as the floor area ratio increases, the total annual solar radiation received by the residential area increases, but the ASU decreases (Figure 7), i.e., the SRA efficiency decreases. This indicates that as the floor area ratio of the residential area increases, the external surface area of the building also increases, so the total amount of solar radiation received by the building increases accordingly but the mutual shading between the buildings will be more serious than before the floor area ratio increases, which leads to the decrease in ASU, i.e., the SRA efficiency decreases.

When the floor area ratio is set as constant, ASU increases as the building height decreases (Figure 7b). Since the floor area ratio is certain, the building density increases when the building height decreases. As a result, ASU increases as the building density increases under the condition of a certain floor area ratio. Therefore, under the condition that the land area and gross floor area are determined, we can increase the annual SRA of the residential area by increasing the building density and decreasing the building height.

Further model calculations show that when the floor area ratio of the residential area increases, whether increasing the building density or increasing the building height, the total annual solar radiation will increase while the annual solar radiation per unit external surface area (ASU) will decrease, but compared to the increase in building height, the

increase in building density will cause the total annual solar radiation to increase faster and the annual solar radiation per unit of external area to decrease more slowly. This indicates that as the building density increases, the roof area of the building will increase, and since it is a homogeneous model and every single building in the residential area is of the same height and uniformly distributed, there is no shading of solar radiation on the roof of the building, which makes the total annual solar radiation obtained from the roof increase. When the building height increases, on the one hand, the annual solar radiation obtained from the roof does not increase because the building roof area remains unchanged, and on the other hand, the increase in building height is more serious than the mutual shading between buildings caused by the increase in building density. Therefore, to have a greater annual SRA, increasing building density is more effective than increasing building height.

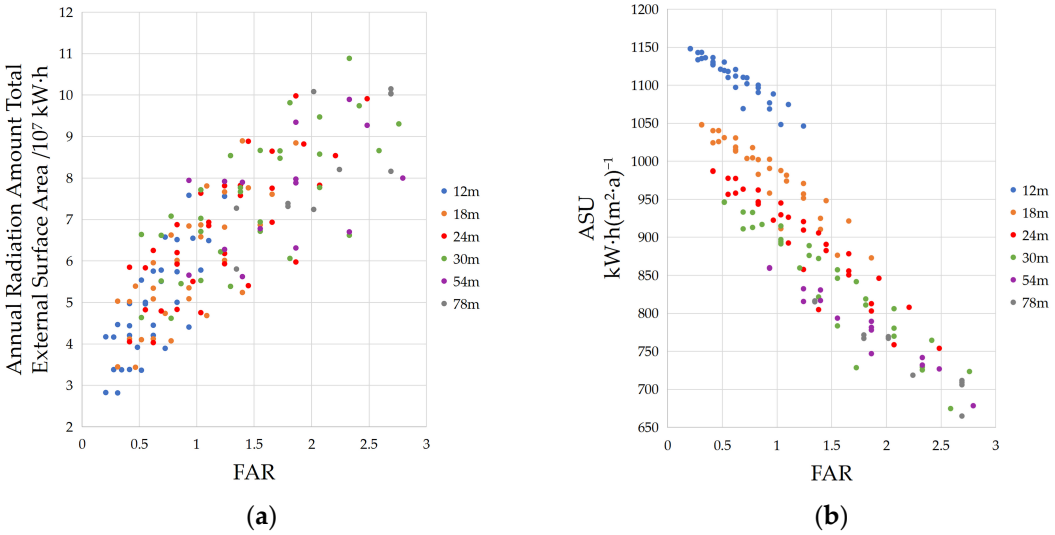


Figure 7. Effect of FAR and BH on annual solar radiation of total external surface area (**a**) and per unit external surface area (ASU) (**b**).

For the heating season SRA, there are also similar conclusions to the annual SRA (Figure 8a,b).

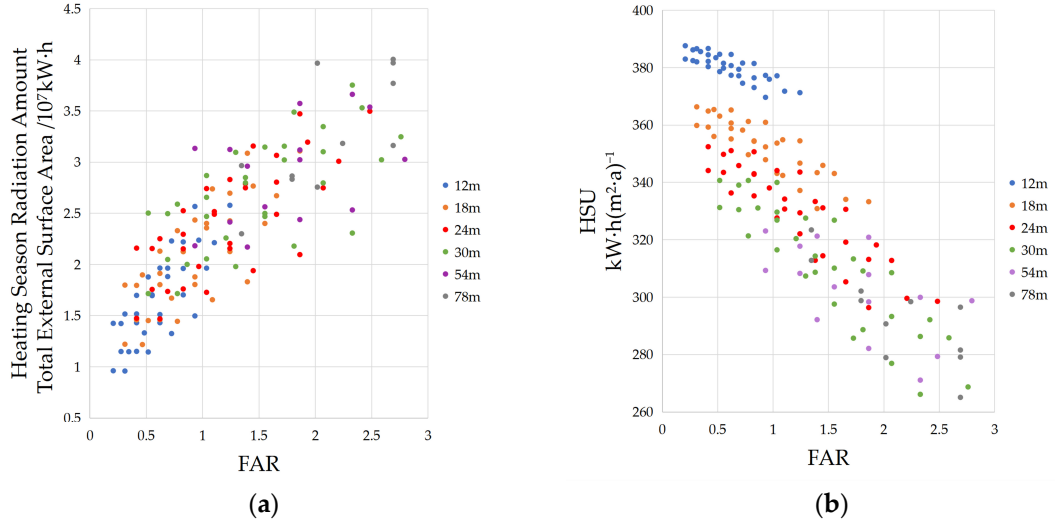
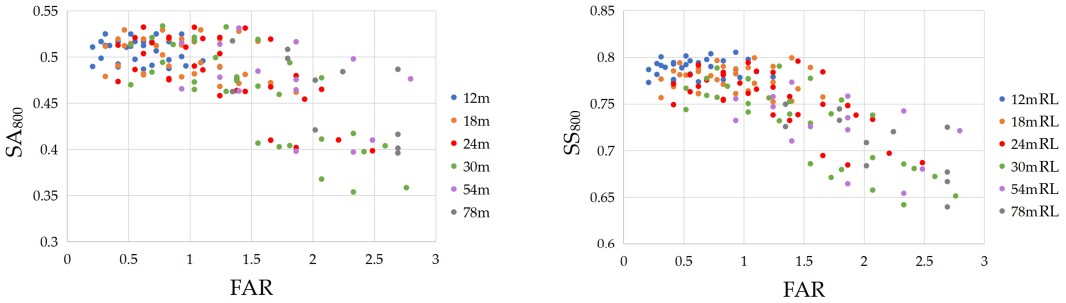


Figure 8. Effect of FAR and BH on heating season solar radiation of total external surface area (**a**) and per unit external surface area (HSU) (**b**).

For the PV potential (SA_{800}, SS_{800}), there are also similar conclusions as for the annual SRA and the heating season SRA (Figure 9). The difference is that in the case of low building height (less than 24 m) and a small floor area ratio (less than 1.5), the changes in both SA_{800} and SS_{800} are small as the floor area ratio increases. However, when the height exceeds 24 m, both SA_{800} and SS_{800} show a significant decreasing trend with the increase in the floor area ratio. It can be seen that in the case of low building height (less than 24 m) and a small floor area ratio (less than 1.5), the radiation mount beyond the 800 threshold can be increased by increasing the building density, thus increasing the PV potential of the residential area.



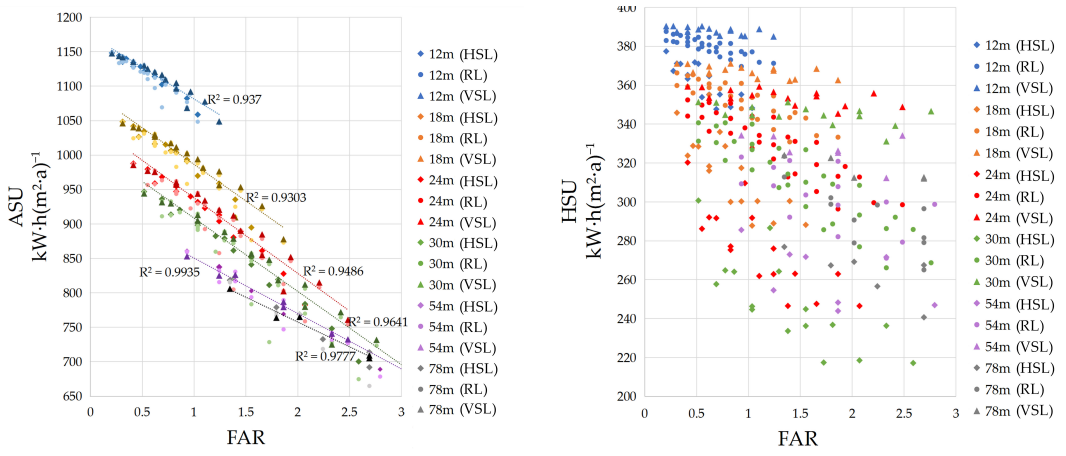
(**a**) (**b**)

Figure 9. Effect of FAR and BH on SA_{800} (**a**) and SS_{800} (**b**).

7.2. Effect of Layout and Building Height (BH) on SRA

The effects of three layout methods (the row layout, the vertical staggered layout, and the horizontal staggered layout) on the SRA and PV potential of the residential area are selected for comparative analysis under due south and due north and six typical building heights.

For SRA, ASU corresponding to all three layouts decreases as the floor area ratio increases (Figure 10a). Among them, the vertical staggered layout performs better than the row and horizontal staggered layout, and the row and horizontal staggered layout are close to each other. In general, the effect of layouts on ASU is not significant.



(**a**) (**b**)

Figure 10. Effect of Layout and BH on ASU (**a**) and HSU (**b**). Note: The HSL represents the horizontal staggered layout; the RL represents the row layout; the VSL represents the vertical staggered layout.

As the floor area ratio increases, HSU decreases for both the row and horizontal staggered layouts (Figure 10b), while there is no significant change in HSU for the vertical staggered layout. Among the three layouts, the vertical staggered layout is the best, followed by the row layout, and the horizontal staggered layout is the worst, while the

vertical staggered layout and the row layout are better than the horizontal staggered layout to a very obvious extent.

Among the three layouts, the vertical staggered layout performs the best in terms of PV potential, while the row layout is very close to it, both of which are significantly better than the horizontal staggered layout (Figures 11 and 12). As the floor area ratio increases, for the same building height, the SA_{800} and SS_{800} of the horizontal staggered layout decrease, while the SA_{800} and SS_{800} of the vertical staggered layout do not change significantly. The row layout is divided into different cases. When the floor area ratio is small (less than 1.5), for the same building height, the SA_{800} and SS_{800} corresponding to the row layout have no significant relationship with the floor area ratio, and when the building height exceeds 24 m and the floor area ratio exceeds 1.5, the SA_{800} and SS_{800} corresponding to the row layout show a significant decreasing trend for the same building height. Further calculation analysis shows that when the floor area ratio is small (less than 1.5), the vertical staggered layout is very close to the row layout, and when the building height exceeds 24 m and the floor area ratio exceeds 1.5, for the same building height, the vertical staggered layout is obviously better than the row layout.

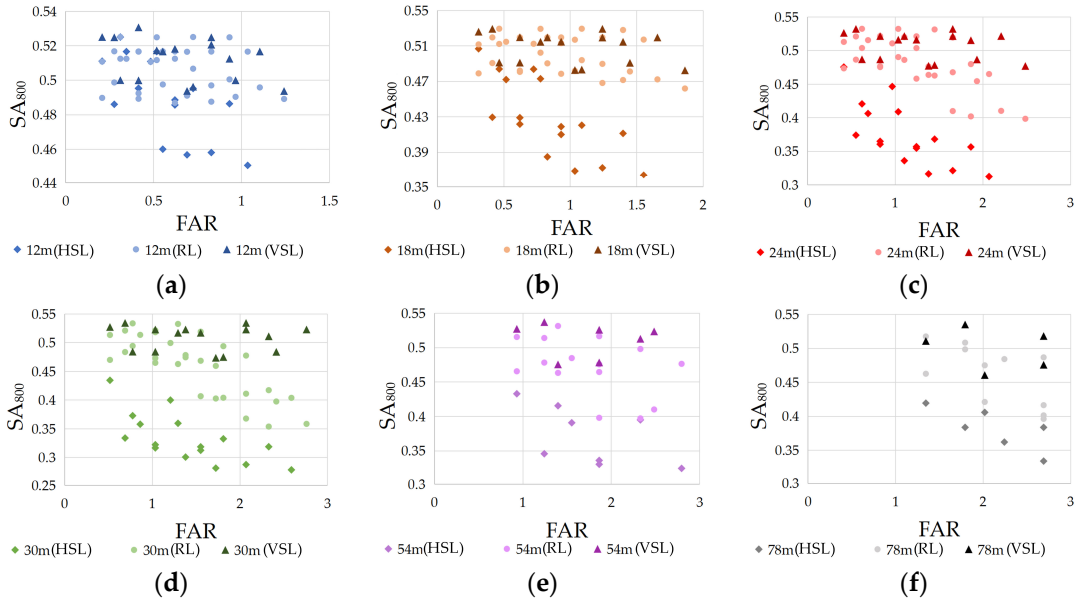


Figure 11. Effect of Layout on SA_{800} under six typical BHs. (**a**) 12 m. (**b**) 18 m. (**c**) 24 m. (**d**) 30 m. (**e**) 54 m. (**f**) 78 m. Note: The HSL represents the horizontal staggered layout; the RL represents the row layout; the VSL represents the vertical staggered layout.

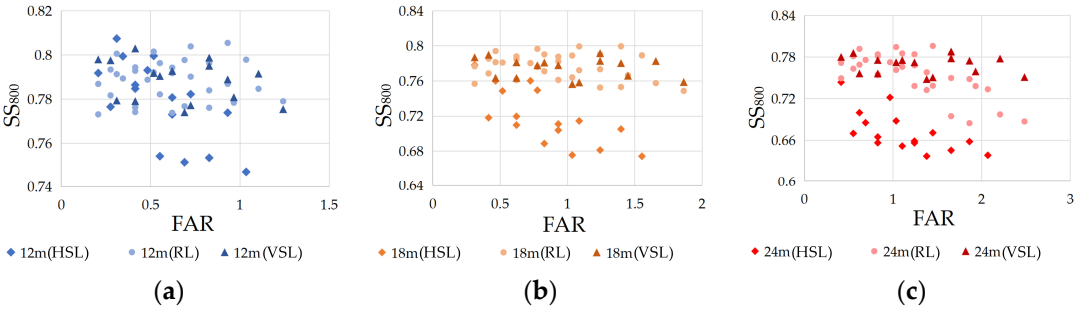


Figure 12. *Cont.*

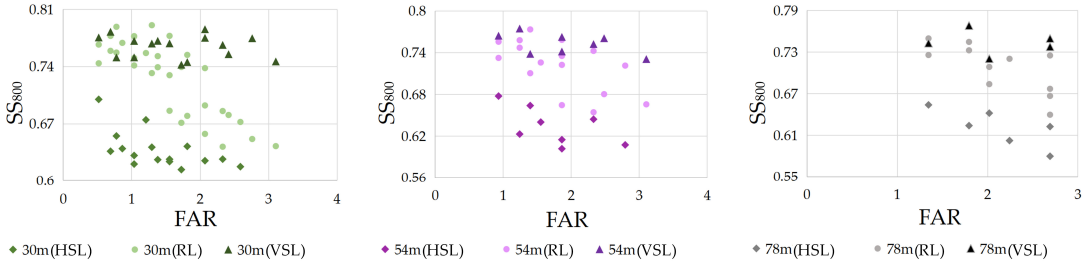


Figure 12. Effect of Layout on SS_{800} under six typical BHs. (**a**) 12 m. (**b**) 18 m. (**c**) 24 m. (**d**) 30 m. (**e**) 54 m. (**f**) 78 m. Note: The HSL represents the horizontal staggered layout; the RL represents the row layout; the VSL represents the vertical staggered layout.

7.3. Effect of Building Orientation (BO) and Building Height (BH) on SRA

The following section selects due south and north as the reference direction of orientation, specifies it as orientation 0°, and the angle formed by counterclockwise rotation is the positive angle, that is, 30° indicates 30° S.E., 60° indicates 60° S.E., 90° indicates due east and west, 120° indicates 60° S.W., 150° indicates 30° S.W., 180° indicates due south and north, 210° indicates 30° S.E., 240° indicates 60° S.E., and 270° indicates due east and west.

Since all the individual buildings in the residential area model are symmetrical slab structures uniformly distributed and of the same height, it is sufficient to study only half of the full 360° orientation range. This is because the solar radiation conditions of the corresponding orientations in the two halves of the orientation range are identical [20]. For example, in the orientation range formed by turning 180° counterclockwise from due south to due north, the solar radiation condition of a building facing 15° S.E. is exactly the same as that of a building facing 15° N.W. in the orientation range formed by turning 180° counterclockwise from due north to due south. The row layout is selected, and Figures 13–16 indicate the SRA of the residential area at different orientations under the row layout, respectively.

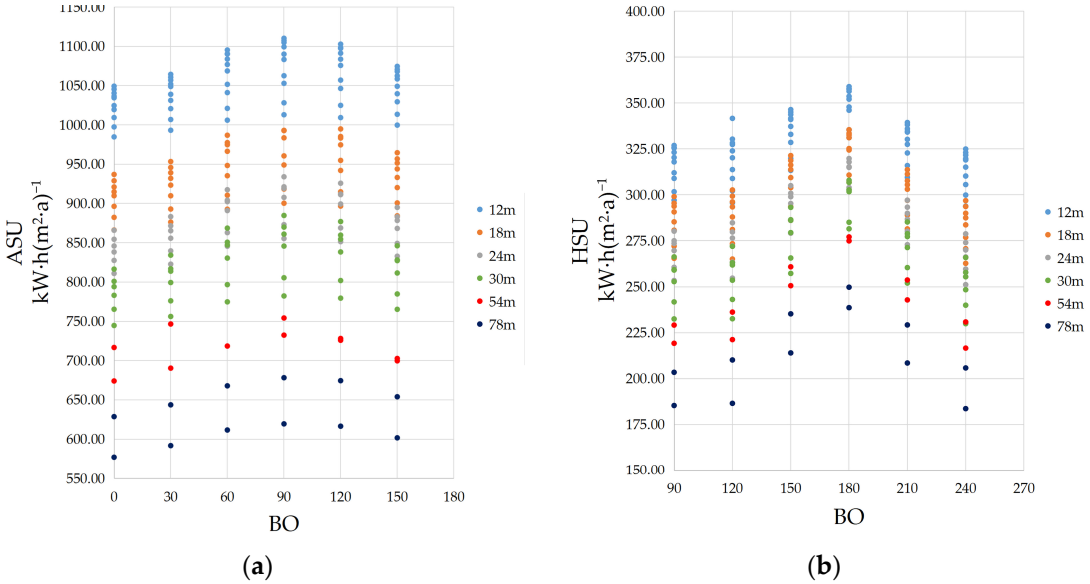


Figure 13. Effect of BO and BH on ASU (**a**) and HSU (**b**).

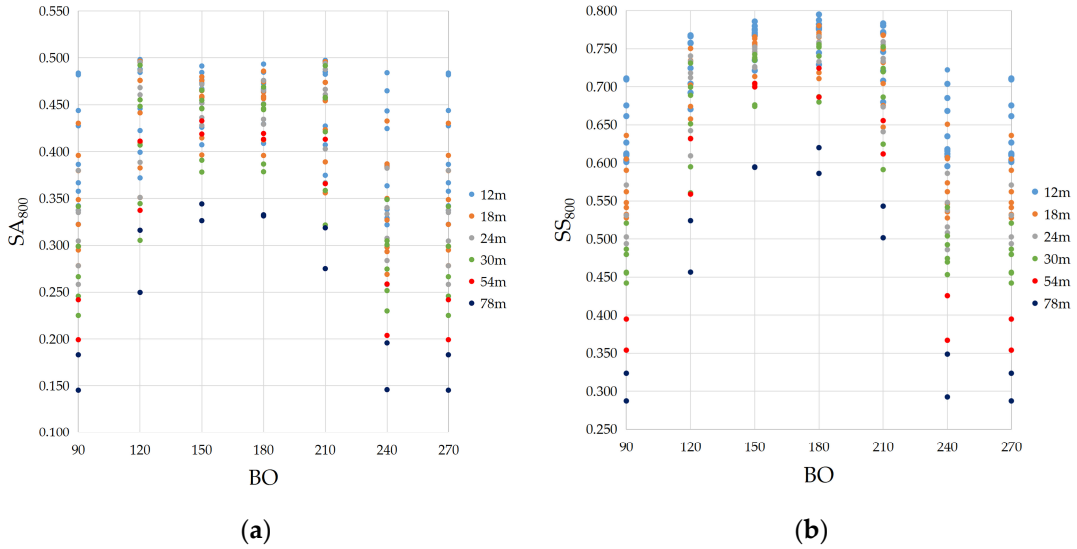


Figure 14. Effect of BO and BH on SA_{800} (**a**) and SS_{800} (**b**).

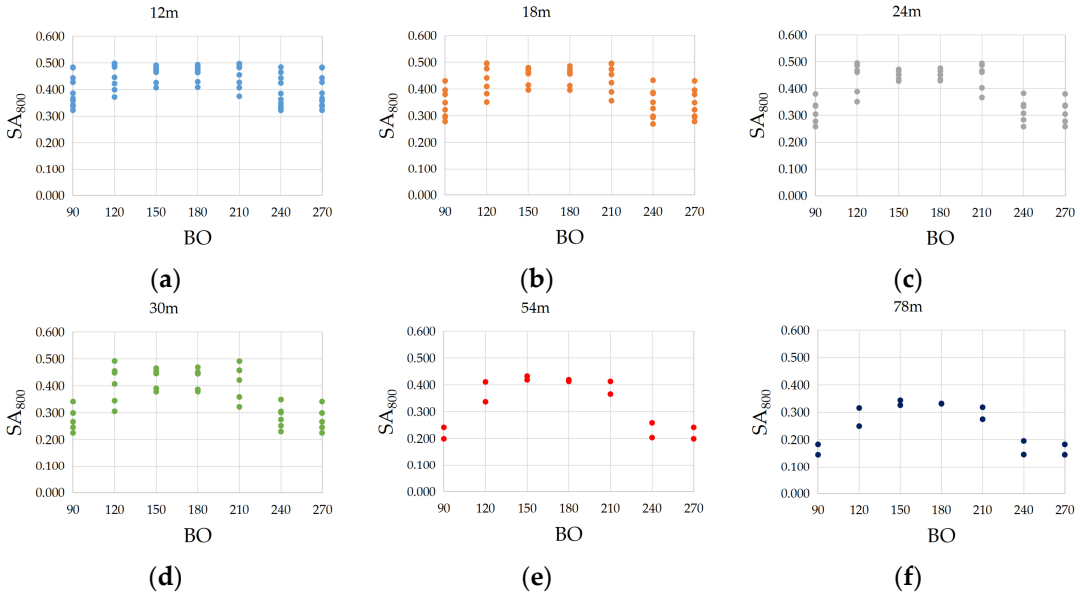


Figure 15. Effect of BO on SA_{800} under six typical BH. (**a**) 12 m. (**b**) 18 m. (**c**) 24 m. (**d**) 30 m. (**e**) 54 m. (**f**) 78 m. Note: the different dot color represents the different BH.

For different building heights, the change pattern of ASU with orientation is basically the same (Figure 13a). When the building orientation is turned 180° counterclockwise from due south (orientation 0°) to due north (orientation 180°), the ASU first increases sequentially and then reaches the maximum value when it is turned near due east (orientation 90°), and then decreases sequentially. Further, the model calculation shows that the optimal ASU orientation range is from 75° S.W. to due west with a span of 15°.

For different building heights, the change pattern of HSU with orientation is also basically the same (Figure 13b). When the building orientation is turned 180° counterclockwise from due east (orientation 90°) to due west (orientation 270°), the HSU first increases sequentially and then reaches the maximum value when it is turned near due north (orientation 180°), and then decreases sequentially. Further, the model calculation shows that the optimal orientation range of HSU is from due south to 10° S.W. with a span of 10°.

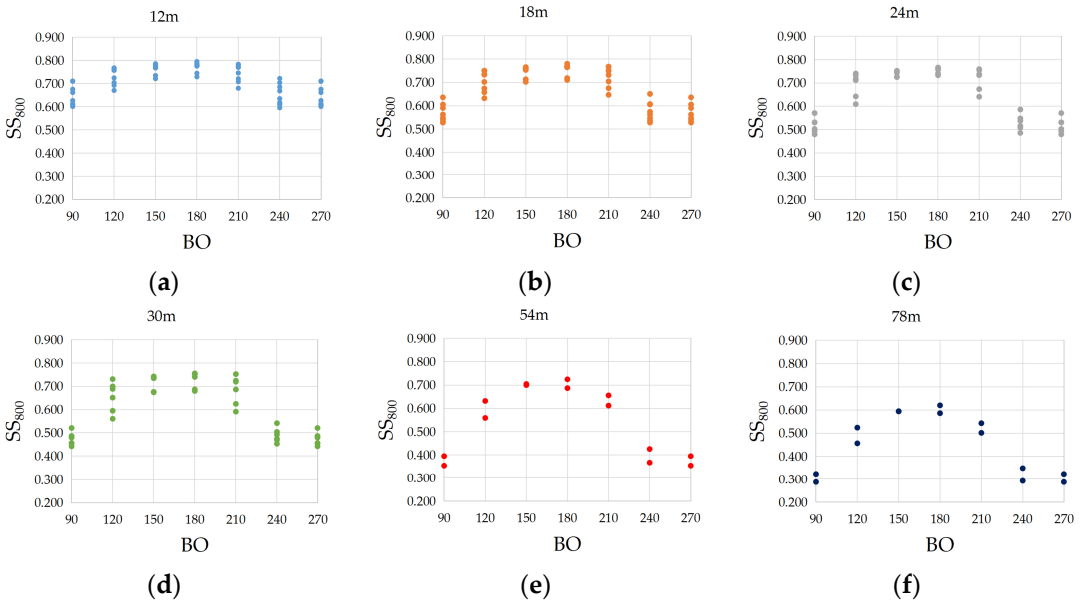


Figure 16. Effect of BO on SS_{800} under six typical BH. (**a**) 12 m. (**b**) 18 m. (**c**) 24 m. (**d**) 30 m. (**e**) 54 m. (**f**) 78 m. Note: the different dot color represents the different BH.

It is interesting to note that ASU and HSU reach their maximum values in opposite directions, with ASU reaching its maximum value near due east and west and its minimum value near due south and north, while HSU reaches its minimum value near due east and west and its maximum value near due south and north.

The influence of building height on PV potential (SA_{800}, SS_{800}) is small, and the changing pattern of PV potential with orientation is basically the same for different heights (Figures 14–16). When the building height is lower than 30 m, SA_{800} is the largest at 60° S.W. and 30° S.E.; when the building height is higher than 30 m, SA_{800} is the largest at 30° S.W. In the process of turning the building orientation 180° counterclockwise from due east to due west, the SS_{800} increases first and then decreases after reaching the peak. The optimal orientation range of the residential area PV potential is from 15° S.W. to 15° S.E. with a span of 30°.

8. Conclusions

In this study, five morphology indexes, including floor area ratio, building height, building density, layout, and building orientation, which can be directly adjusted by architects during the design process are selected. The study compares the sensitivity of these multiple morphology indexes when changed collectively and assesses their comprehensive impact on the SRA potential of residential areas. Using comprehensive comparative analysis of Lhasa urban residential area morphology indexes based on the SRA potential, the results show that:

1. When considering the floor area ratio index under the condition that the land area and gross floor area are determined, an increase in building density proves more advantageous for enhancing SRA compared to an increase in building height. In cases where the building height is less than 24 m and the floor area ratio is below 1.5, elevating the building density yields greater photovoltaic (PV) potential for the residential area.
2. With a limited site area, the impact of building height on SRA far outweighs that of the layout. The layout does not significantly affect the annual solar radiation amount per unit of external surface area (ASU). With increasing building height, the impact of layout on heating season solar radiation amount per unit external surface area (HSU) becomes more pronounced. The vertical staggered layout and the row layout exhibit significantly superior performance compared to the horizontal staggered layout in

this regard. However, when the building height exceeds 24 m and the floor area ratio surpasses 1.5, the PV potential of the vertical staggered layout surpasses that of the row layout and the horizontal staggered layout for the same building height.

3. For building orientation and building height, building height has a slightly greater effect on SRA than orientation. The change pattern of the same SRA index with orientation is basically the same under different heights. Among them, the best orientation range of annual SRA is from 75° S.W. to due west with a span of 15°, the best orientation range of heating season SRA is from due south to 10° S.W. with a span of 10°, and the best orientation range of PV potential is from 15° S.W. to 15° S.E. with a span of 30°. The optimal orientation of annual SRA is the opposite of the optimal orientation of heating season SRA.

There are still some limitations to this study, which should be studied in the future:

1. The study has a limited geographical scope, focusing solely on the residential areas of Lhasa. The applicability of the conclusions under multiple climate zones will be investigated based on a larger sample in follow-up studies.
2. The study solely concentrates on the residential buildings within the residential area, taking little consideration of the presence and impact of nearby public buildings. The interrelationship between these residential buildings and public buildings is not taken into consideration. In future research, it would be valuable to expand the scope of the investigation to include public buildings within residential areas. Examining how public buildings shade neighboring residential buildings from solar radiation can provide a more precise analysis of the correlation between residential area morphology and SRA potential.
3. In this study, the utility of the BP neural network for predicting residential area SRA potential has been affirmed, which is a widely applicable research pathway for investigating the relationship between residential area morphology design and SRA potential in any climate zone. The subsequent research will focus on expanding the training sample set and condensing the summary of research findings even further, which will further improve the accuracy to reach the ideal state and thus provide more convenient, intuitive, and accurate guidance for the design phase.

Author Contributions: G.S., Y.L., W.L., J.T. and S.C. conceived the paper; G.S. and W.L. performed the field measurement and investigation; G.S. analyzed the data and drafted the paper; G.S., Y.L. and W.L. revised the paper. All authors have read and agreed to the published version of the manuscript.

Funding: This research was funded by the National Natural Science Foundation of China, grant number 52078422.

Institutional Review Board Statement: Not applicable.

Informed Consent Statement: Not applicable.

Data Availability Statement: Data are contained within the article.

Acknowledgments: We want to thank the editor and anonymous referees for their kind help. We also thank our research group for their discussion and inspiration in the early stage of this study.

Conflicts of Interest: Wenqiang Li was employed by the Digitalize Civil Branch of China Railway 12th Bureau Co., Ltd. The remaining authors declare that the research was conducted in the absence of any commercial or financial relationships that could be construed as a potential conflict of interest.

References

1. Zou, Y.; Deng, Y.; Xia, D.; Lou, S.; Yang, X.; Huang, Y.; Guo, J.; Zhong, Z. Comprehensive analysis on the energy resilience performance of urban residential sector in hot-humid area of China under climate change. *Sustain. Cities Soc.* **2023**, *88*, 104233. [CrossRef]
2. Nie, H.; Kemp, R.; Fan, Y. Investigating the adoption of energy-saving measures in residential sector: The contribution to carbon neutrality of China and Europe. *Resour. Conserv. Recycl.* **2023**, *190*, 106791. [CrossRef]
3. Mostafa, N.A.; Grida, M.; Park, J.; Ramadan, H.S. A sustainable user-centered application for residential energy consumption saving. *Sustain. Energy Technol. Assess.* **2022**, *53*, 102754. [CrossRef]

4. Song, S. *Climate in Tibet*; China Meteorological Press: Beijing, China, 2013; p. 512.
5. Yan, J. Study on roof inclination of buildings at high altitude based on solar radiation-taking Lhasa as an example. *Intell. Build. Smart City* **2023**, 104–106. [CrossRef]
6. Lu, M.; Du, J. Assessing the daylight and sunlight availability in high-density residential areas: A case in North-east China. *Archit. Sci. Rev.* **2013**, *56*, 168–182. [CrossRef]
7. Košir, M.; Capeluto, I.G.; Krainer, A.; Kristl, Ž. Solar potential in existing urban layouts—Critical overview of the existing building stock in Slovenian context. *Energy Policy* **2014**, *69*, 443–456. [CrossRef]
8. Martins, T.A.; Adolphe, L.; Bastos, L.E. From solar constraints to urban design opportunities: Optimization of built form typologies in a Brazilian tropical city. *Energy Build.* **2014**, *76*, 43–56. [CrossRef]
9. Sarralde, J.J.; Quinn, D.J.; Wiesmann, D.; Steemers, K. Solar energy and urban morphology: Scenarios for increasing the renewable energy potential of neighbourhoods in London. *Renew. Energy* **2015**, *73*, 10–17. [CrossRef]
10. Zhu, R.; Wong, M.S.; You, L.; Santi, P.; Nichol, J.; Ho, H.C.; Lu, L.; Ratti, C. The effect of urban morphology on the solar capacity of three-dimensional cities. *Renew. Energy* **2020**, *153*, 1111–1126. [CrossRef]
11. Liu, Y. Research on Design Guidance and Control of Solar Energy Utilization in Urban Residential Buildings in Lanzhou. Master's Thesis, Northwestern Polytechnical University, Xi'an, China, 2020.
12. Chen, R. Study on the Influence of Residential Morphology on Solar Radiation. Master's Thesis, Xi'an University of Architecture and Technology, Xi'an, China, 2021.
13. Wu, Z.; Ren, Y.; Chen, L. Evaluating Urban Geometry Impacts on Incident Solar Radiation on Building Envelopes. *Environ. Model. Assess.* **2021**, *26*, 113–123. [CrossRef]
14. Tian, J.; Xu, S. A morphology-based evaluation on block-scale solar potential for residential area in central China. *Sol. Energy* **2021**, *221*, 332–347. [CrossRef]
15. Wen, T. Study on the Influence of Urban Residential Pattern Layout on Solar Energy Utilization Potential in Xining. Master's Thesis, Northwestern Polytechnical University, Xi'an, China, 2021.
16. Boccalatte, A.; Thebault, M.; Ménézo, C.; Ramousse, J.; Fossa, M. Evaluating the impact of urban morphology on rooftop solar radiation: A new city-scale approach based on Geneva GIS data. *Energy Build.* **2022**, *260*, 111919. [CrossRef]
17. Yi, Z.Z. Research on Energy Saving Optimization Design of Space form of Near Zero Energy Residential Area under the Influence of Solar Radiation. Master's Thesis, Shandong Jianzhu University, Jinan, China, 2023.
18. Vermeulen, T.; Knopf-Lenoir, C.; Villon, P.; Beckers, B. Urban layout optimization framework to maximize direct solar irradiation. *Comput. Environ. Urban Syst.* **2015**, *51*, 1–12. [CrossRef]
19. Li, D.; Liu, G.; Liao, S. Solar potential in urban residential buildings. *Sol. Energy* **2015**, *111*, 225–235. [CrossRef]
20. Morganti, M.; Salvati, A.; Coch, H.; Cecere, C. Urban morphology indicators for solar energy analysis. *Energy Procedia* **2017**, *134*, 807–814. [CrossRef]
21. Bai, Y. Study on Optimization of Residential form in Cold Regions Based on Solar Energy Utilization Potential. Master's Thesis, Harbin Institute of Technology, Harbin, China, 2017.
22. Jiang, N. Solar Potential Assessment of Residential Areas—A Case Study of Wuhan. Master's Thesis, Huazhong University of Science and Technology, Wuhan, China, 2018.
23. Aghamolaei, R.; Ghaani, M.R.; Tahsildoost, M.; Zandi, M. A comprehensive energy-oriented approach for optimization of solar potential in urban contexts: An application study for residential districts. *Adv. Build. Energy Res.* **2019**, *13*, 205–219. [CrossRef]
24. Zhang, J.; Xu, L.; Shabunko, V.; Tay, S.E.R.; Sun, H.; Lau, S.S.Y.; Reindl, T. Impact of urban block typology on building solar potential and energy use efficiency in tropical high-density city. *Appl. Energy* **2019**, *240*, 513–533. [CrossRef]
25. Zhang, H. Study on the Relationship between Solar Radiation Utilization and Residential Layout in Lhasa City Collective Housing. Master's Thesis, Xi'an University of Architecture and Technology, Xi'an, China, 2021.
26. Shi, J.; Zhou, Y.; Ma, Y.; Zhu, D. Research on Construction and Application of Solar Energy Potential Forecast Model in Residential Areas. *Hous. Sci.* **2019**, *39*, 53–58.
27. Bai, Y.; Ma, T. Experimental study on solar energy utilization potential of building surface in Matao City of Harbin. *Shanxi Archit.* **2017**, *43*, 177–179.
28. Chen, Y. Analysis of Current Situation and Optimization Strategy of Solar Energy Access in Residential Areas of Harbin. Master's Thesis, Harbin Institute of Technology, Harbin, China, 2016.
29. Zhang, Y. Study on the Influence of Planning and Layout of High-Rise Residential Areas on Solar Radiation Acquisition in Harbin. Master's Thesis, Harbin Institute of Technology, Harbin, China, 2019.
30. Li, C. Spatial Analysis of Photovoltaic Utilization and Its Development Potential in Harbin High-Rise Residential Areas. Master's Thesis, Harbin Institute of Technology, Harbin, China, 2018.
31. Zhu, D.; Song, D.; Shi, J.; Fang, J.; Zhou, Y. The Effect of Morphology on Solar Potential of High-Density Residential Area: A Case Study of Shanghai. *Energies* **2020**, *13*, 2215. [CrossRef]
32. Zhu, D.; Song, D.; Shi, J. Effects of Residential District Density Parameters on Solar Potential—A Comparative Study between Beijing and Shanghai. In Proceedings of the 14th International Green Building and Building Energy Efficiency Conference and New Technology and Product Expo, Shenzhen, China, 2 April 2018.

33. Zhu, D.; Song, D.; Shi, J. Characteristics of Solar Radiation Received from the Outer Surface of High-Density Residential Buildings. In Proceedings of the Fifteenth International Conference on Green and Energy-Efficient Building & New Technologies and Products Expo, Shenzhen, China, 3 April 2019.
34. Wu, J.; Liang, X.; Yu, B.; Jin, J.; Wang, D. Research on the Application of BP Artificial Neural Network in DSM Comprehensive Evaluation. *Green Constr. Intell. Build.* **2016**, 51–55.
35. Hao, S. Study on the Influence of Flat Facade Morphology on Solar Radiation Receiving Potential of Building Facade. Master's Thesis, Northwestern Polytechnical University, Xi'an, China, 2022.
36. Li, W. Research on the Guidance and Control Indexes for the Morphology Design of Residential Area Based on Solar Energy Acquisition Potential- Take Lhasa City as an Example. Master's Thesis, Northwestern Polytechnical University, Xi'an, China, 2023.
37. Compagnon, R. Solar and daylight availability in the urban fabric. *Energy Build.* **2004**, *36*, 321–328. [CrossRef]

Disclaimer/Publisher's Note: The statements, opinions and data contained in all publications are solely those of the individual author(s) and contributor(s) and not of MDPI and/or the editor(s). MDPI and/or the editor(s) disclaim responsibility for any injury to people or property resulting from any ideas, methods, instructions or products referred to in the content.